White lines and d-electron occupancies for the $3d$ and $4d$ transition metals

D. H. Pearson,* C. C. Ahn, and B. Fultz
California Institute of Technology, Division of Engineering of Applied Science, Mail Code 138-78, Pasadena, California 91125
(Received 27 July 1992; revised manuscript received 30 November 1992)

We used electron-energy-loss spectrometry to measure the intensities of the white lines found at the onsets of the L_2 and L_3 absorption edges for most of the $3d$ and $4d$ transition metals. The intensities of the white lines, normalized to the trailing background, decreased nearly linearly with increasing atomic number, reflecting the filling of the d states. One-electron Hartree-Slater calculations of the white-line intensities were in good agreement with observed spectra. Empirical correlations between normalized white-line intensity and d-state occupancy provide a method for measuring changes in d-state occupancy due to alloying.

I. INTRODUCTION

Some of the most distinctive features observed in the electron-energy-loss spectra (EELS) and x-ray-absorption spectra (XAS) of transition metals are the peaks known as "white lines" found at the onsets of the L_2 and L_3 absorption edges. These peaks, which are quite intense for the early transition metals of each transition series, were first correctly interpreted by Mott[1] as being due to excitations of $2p$ core electrons in an atom to unoccupied d-like states near the Fermi level. The peaks have been called white lines because they were originally observed as overexposed regions on the photographic film originally used to record x-ray-absorption spectra.[2]

A number of EELS and XAS studies based upon the one-electron approximation have attempted to relate changes in total white-line intensities observed during compound formation to changes in the occupancies of the corresponding outer d states. Lytle *et al.*[3] compared L_3 white-line intensities for a number of Ir, Pt, and Au compounds with those of the respective pure metals and concluded that the differences in the white-line intensities reflected changes in the occupancies of the local $5d$ states that were due to compound formation. White-line intensities for Pt and Ir were also studied by Horsley[4] and later by Mansour, Cook, and Sayers[5] who relied upon band-structure calculations to calibrate the white-line intensities. Using a similar approach, Sham, Tan, and Yiu[6–8] determined changes in the occupancies of the outer d states for a number of Au, Pd, and Ni compounds. In addition, tight-binding calculations for Pt by Brown, Peierls, and Stern[9] and Mattheiss and Dietz[10] predicted a modest white line at the Pt L_3 absorption edge due to the presence of $j=\frac{5}{2}$ d holes, in agreement with observed spectra.

Other studies have focused on the ratio of the L_3 white-line intensity to the L_2 white-line intensity. Leapman and Grunes[11] pointed out that the observed ratios did not follow the expected 2:1 ratio for the early $3d$ transition metals. Zaanen *et al.*[12] later showed that these anomalous ratios could be partially explained by atomic multiplet effects which cause overlapping transitions from $2p_{1/2}$ and $2p_{3/2}$ states. Atomic multiconfigurational calculations of Waddington *et al.*[13] also predicted anomalous ratios. In spite of these difficulties, however, it appears that measurements of white-line ratios may be used to investigate the angular momentum character of outer d states in transition-metal alloys.[14,15] Another difficulty, discussed by Stern and Rehr,[16] is the use of the one-electron approximation itself. They suggested that many-body effects under the influence of the core hole may be significant in interpreting the structure at absorption edges. They showed, however, that the many-body problem reduces to an effective one-electron problem for transitions to an initially empty shell, or for transitions that fill a shell.

In this work we present an experimental EELS study of the white lines for the elements of the $3d$ and $4d$ transition series. This work builds upon a previous EELS study[17] in which we reported an empirical method for measuring changes in the $3d$-state occupancy of transition-metal atoms upon alloying. We also present Hartree-Slater calculations of the white-line intensities for the elements of both transition series and show that EELS in the transmission electron microscope may be used to probe the occupancies of the outer d states of transition-metal atoms.

This work is organized as follows. In Sec. II, the sample preparation, data acquisition, and data processing are described. An analysis of the spectra is presented in Sec. III. In Sec. IV, the calculations are presented and are compared to the experimental spectra. A discussion of the results in terms of their application to measuring changes in d-state occupancy upon alloying is presented in Sec. V. Conclusions are given in Sec. VI.

II. EXPERIMENT

Electron-transparent samples of most $3d$ and $4d$ transition metals were prepared for energy-loss analysis in the transmission electron microscope (TEM). For some specimens, disks 3 mm in diameter were cut from nominally pure, thin foils and were then electrochemically polished. For other specimens, thin films were prepared by thermal evaporation, electron-beam evaporation, or direct-current argon-ion sputtering onto single-crystal

NaCl substrates. These films were then floated off the substrates in water and picked up with Cu TEM grids.

Samples of the $3d$ metals were analyzed with a Gatan 607 serial-detection electron-energy-loss spectrometer on a Philips EM 430 TEM in diffraction mode at 200 kV using a camera length of 80 mm and a spectrometer collection aperture of 3 mm. All spectra were examined for oxygen edges, and when necessary samples were ion milled to remove any surface oxides. These spectra were then deconvoluted by the Fourier-log method[18] to remove multiple-scattering components from the spectra and were background-subtracted by fitting the preedge background with a power-law function.[19]

Samples of the $4d$ metals were analyzed with a Gatan 666 parallel-detection electron-energy-loss spectrometer on the Philips EM 430 TEM in image mode with no objective aperture and a 3-mm spectrometer collection aperture. Since the Gatan 666 spectrometer collects only 1024 channels of data simultaneously, the low-loss and core-loss spectra were collected separately. These spectra required further processing before deconvolution owing to the response function and gain fluctuations of the photodiode-array detector.[20] Specifically, several spectra were collected for both the low-loss and the core-loss regions, each shifted by a few data channels from the previous spectrum. These data were then divided by the response function determined by uniformly illuminating the photodiode array with no sample in place. The individual spectra were then realigned to a common feature in the spectrum and added. This latter step reduces noise by averaging the channel-to-channel gain fluctuations of the detector. The spectra were then background-subtracted and deconvoluted by the Fourier-ratio method.[21]

III. ANALYSIS OF SPECTRA

The deconvoluted and background-subtracted $L_{2,3}$ energy-loss spectra for the $3d$ transition metals are shown in Fig. 1. The corresponding data for the $4d$ transition metals are shown in Fig. 2. In order to present all the spectra of a given transition series on the same figure, the characteristic edge energies are not shown. For comparison, the spectra have been scaled such that their background intensities past the L_2 edge are approximately equal. Note how the white lines at the L_2 and L_3 edge onsets decrease in intensity with increasing Z across each series, reflecting the filling of the outer d states.

To address quantitatively the relationship between the white-line intensity and the number of d holes, we consider the sum of the areas in the white lines. Mattheiss and Dietz[10] have shown, using an atomic, one-electron model, that the areas A_2 and A_3 under the L_2 and L_3 white lines, respectively, are given by

$$A_3 = KR_{2p_{3/2}}\left(\tfrac{2}{5}h_{5/2} + \tfrac{1}{15}h_{3/2}\right) \quad (1)$$

and

$$A_2 = KR_{2p_{1/2}}\left(\tfrac{1}{3}h_{3/2}\right) . \quad (2)$$

Here $h_{3/2}$ and $h_{5/2}$ are the numbers of $j=\frac{3}{2}$ and $\frac{5}{2}$ d holes, $R_{2p_{3/2}}$ and $R_{2p_{1/2}}$ are the radial matrix elements for the excitations of the $2p_{3/2}$ and $2p_{1/2}$ core electrons, and K is a normalization constant. The expressions were evaluated using dipole selection rules while ignoring excitations to outer s states, since the matrix elements for these transitions are much smaller than those for excitations to d states. Taking $R_{2p_{3/2}}$ and $R_{2p_{1/2}}$ to be approximately equal, and denoted R_{2p}, the sum of the areas under the white lines is given by

$$A_{\text{total}} = KR_{2p}\tfrac{6}{15}(h_{3/2}+h_{5/2}) \propto R_{2p}h_{\text{total}} . \quad (3)$$

Thus, the sum of the white-line areas is expected to be proportional to the total number of d holes, h_{total}.

One must be careful, however, to define what exactly is meant by d holes (or alternatively, d occupancy) in the context of absorption spectra measurements.[22,23] As an example, Ni is known to have 9.4 electrons in the $3d$ band.[24,25] These electrons, however, possess a small amount of $4s$ character due to hybridization such that the actual $3d$ character only constitutes 8.8 electrons.[26] In L_2 and L_3 absorption spectra, the initial $2p$ states couple

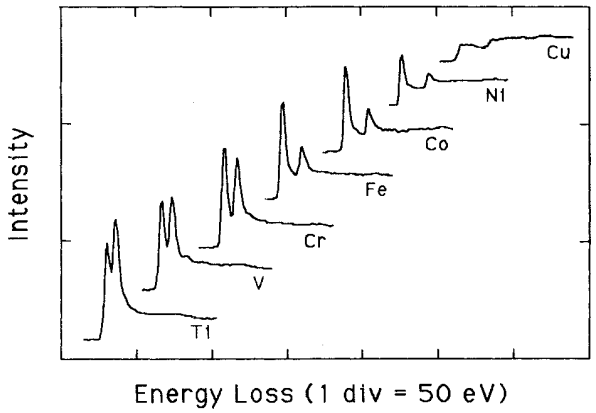

FIG. 1. Background-subtracted and deconvoluted $L_{2,3}$ edges for the $3d$ transition metals.

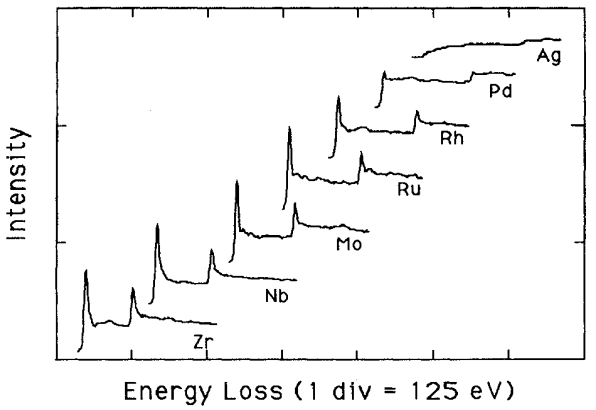

FIG. 2. Background-subtracted and deconvoluted $L_{2,3}$ edges for the $4d$ transition metals.

predominantly to the states with $3d$ (or $4d$) character. Thus in this context, the d occupancy or d count for Ni is 8.8 electrons.

To establish the numerical proportionality between white-line intensity and the number of d holes for the transition metals, the white lines must be isolated from the background intensity and normalized. Figure 3 for Mo illustrates our empirical method for isolating and normalizing the white lines in spectra for the $4d$ transition metals. The background intensity was modeled by step functions in the threshold regions since the L_2 and L_3 edges for Ag, which has no white lines, resemble step functions. A straight line over a range of approximately 50 eV was fit to the background intensity immediately following each white line. This line was then extrapolated into the threshold region and set to zero at energies below that of the white-line maximum. The L_2 white line was further isolated by smoothly extrapolating the L_3 background intensity under the L_2 edge. The areas in the white lines were added and then divided by the area in a normalization window 50 eV in width beginning 50 eV past the L_3 white-line onset. Because the optimum x-axis position for the step functions is somewhat uncertain, we also repeated the analysis after shifting the step functions to lower energy such that they intersected the rising edge of the white lines.

Plots of the normalized white-line intensity versus $4d$ occupancy for each choice of step-function position is shown in Fig. 4. The occupancy of the $4d$ states was determined by assuming a valence electron configuration of $4d^{N-1}s^1$, where N is the total number of valence electrons, as this is approximately the configuration in the solid.[27] As mentioned above, hybridization will slightly alter the amount of d character from integer values. To our knowledge, however, calculations of the amount of d character as defined above have not been reported for all of the $3d$ and $4d$ transition metals, so for consistency we used the integer values. Since the $4d$ occupancy increases nearly linearly across the $4d$ transition series, one might

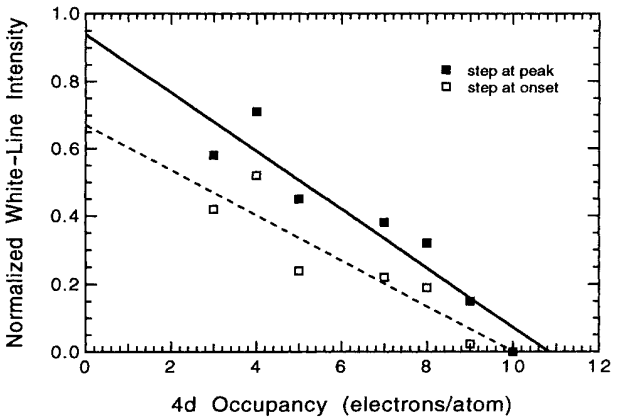

FIG. 4. Plot of normalized white-line intensity vs $4d$ occupancy. Linear fits to the data give $I=0.94(1-0.092n)$ for the upper curve (steps at peaks) and $I=0.67(1-0.10n)$ for the lower curve (steps at onsets).

expect a linear decrease in the normalized white-line intensity. Furthermore, if the normalized white-line intensity, I, depended solely upon the $4d$ occupancy, n, the expected correlation would be

$$I=K(1-0.1n)\,, \tag{4}$$

so the intensity would be a maximum at $n=0$ and go to zero at $n=10$. The constant, K, is arbitrary and depends upon the specific normalization scheme. The linear fits obtained from the data in Fig. 4 are

$$I_{4d}=0.94(1-0.092n_{4d}) \text{ for steps at peaks} \tag{5}$$

and

$$I_{4d}=0.67(1-0.10n_{4d}) \text{ for steps at onsets}\,. \tag{6}$$

We used a similar approach in the analysis of the $3d$ metals, as illustrated for V in Fig. 5. In this more difficult case, the white lines were isolated by modeling the background with a double step function. A straight line was fit to the background immediately following the L_2 white

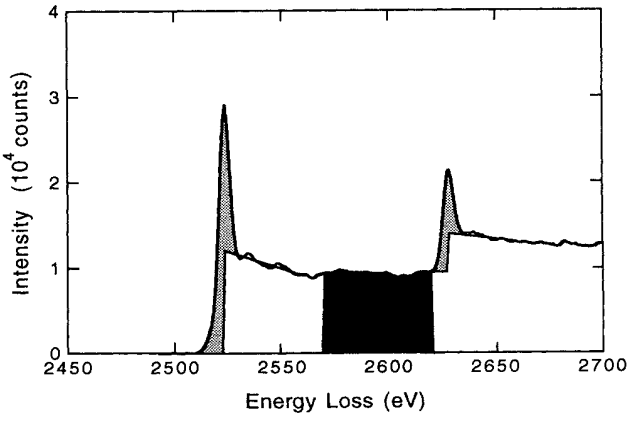

FIG. 3. $L_{2,3}$ edge for Mo showing our method for isolating and normalizing the white-line intensities for the $4d$ transition metals.

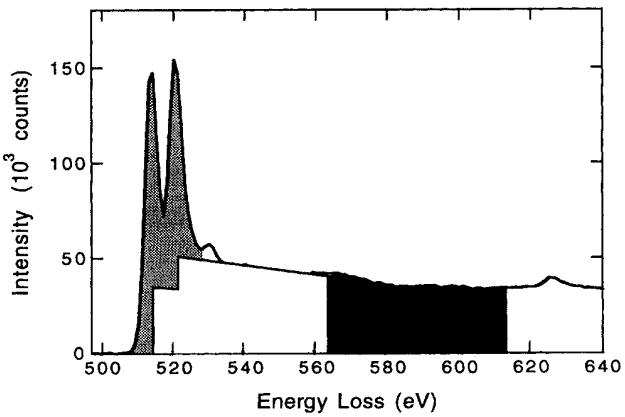

FIG. 5. $L_{2,3}$ edge for V showing our method for the isolating and normalizing the white-line intensities for the $3d$ transition metals.

line over a region of approximately 50 eV and was then extrapolated into the threshold region. This line was then modified into a double step of the same slope with onsets occurring at the white-line maxima. The ratio of the step heights was chosen as 2:1 in accordance with the multiplicity of the initial states (four $2p_{3/2}$ electrons and two $2p_{1/2}$ electrons). This assumption for the step-height ratio may break down for the early $3d$ transition metals, as the intensities of the white lines are expected to deviate from the 2:1 ratio.[11] Since the exact ratio is unknown, however, the 2:1 ratio was used for consistency. The white-line area above this step function was then divided by the area in a normalization window 50 eV in width beginning 50 eV past the onset of the L_3 white line. The analysis was also repeated after shifting the step function to lower energy such that it intersected the rising edge of the white line. Plots of the normalized white-line intensity versus $3d$ occupancy for each choice of step-function position, assuming a $3d^{N-1}s^1$ valence-electron configuration, are shown in Fig. 6. The linear fits obtained from the data are

$$I_{3d}=1.06(1-0.094n_{3d}) \text{ for steps at peaks} \quad (7)$$

and

$$I_{3d}=0.93(1-0.095n_{3d}) \text{ for steps at onsets} . \quad (8)$$

From the plots in Figs. 4 and 6 it is apparent that there is less uncertainty in the normalized white-line intensity for the $3d$ metals than for the $4d$ metals. This is not surprising considering that the white lines for the $3d$ metals are relatively sharper and more intense than those for the $4d$ metals. The difference in the white-line shapes may be explained in part by the wider d band for the $4d$ metals and by the better energy resolution (full width at half maximum of the zero-loss peak) for the $3d$ data (FWHM$\approx$2 eV for the $3d$ data and FWHM$\approx$3 eV for the $4d$ data). As a result, the percent change in white-line area after shifting the step functions is larger for the $4d$ metals. Solid-state calculations of the L_2 and L_3 edge intensities resolved according to final angular momentum states could provide a more accurate means for isolating the white lines, but such calculations were beyond the scope of this paper.

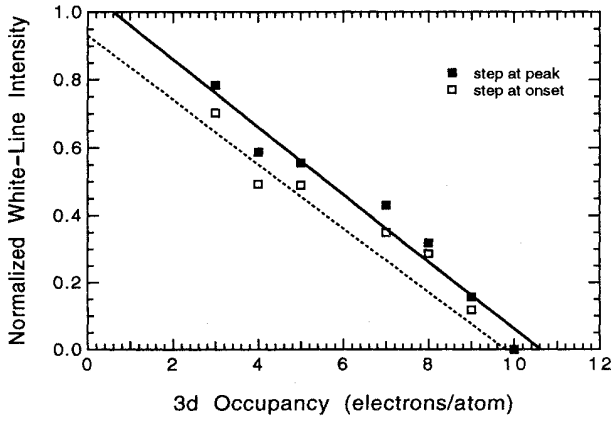

FIG. 6. Plot of normalized white-line intensity vs $3d$ occupancy. Linear fits to the data give $I=1.06(1-0.094n)$ for the upper curve (steps at peaks) and $I=0.93(1-0.095n)$ for the lower curve (steps at onsets).

The correlations in Figs. 4 and 6 are potentially useful for determining changes in outer d state occupancy upon alloying or during solid-state phase transformations if corresponding changes in the normalized white-line intensity are observed. For example, if a 5% enhancement in the normalized intensity was observed after alloying for a $3d$ atom species, the upper curve in Fig. 6 would suggest that about 0.5 electron/atom had left the $3d$ states of that atom species. Using Figs. 4 and 6 for such measurements, however, ignores the contribution of the transition matrix elements to the total intensity. The evaluation of this contribution using atomic, one-electron calculations is the subject of the next section.

IV. CALCULATIONS

The normalized intensity plotted in Figs. 4 and 6 is not only a function of the number of d holes, but also depends upon the radial matrix elements [Eq. (3)] and the background intensity to which the white lines are normalized. The significance of these factors should therefore be evaluated.

For ionizing transitions to the continuum, the measured intensity in an energy-loss spectrum is proportional to the energy-differential cross section, $d\sigma/dE$,[28,29] given in the first Born approximation by

$$\frac{d\sigma}{dE}=\frac{8\pi\hbar^2}{a_0^2 m_0^2 v^2}\int_{q_{\min}}^{q_{\max}}\frac{1}{q^3}|\langle f|e^{i\mathbf{q}\cdot\mathbf{r}}|i\rangle|^2 dq . \quad (9)$$

Here $\mathbf{r}$ is the position vector of the incident electron, a_0 is the Bohr radius, m_0 is the rest mass of the electron, v is the speed of the incident electron, $\mathbf{q}$ is the change in wave vector of the incident electron, and $|i\rangle$ and $|f\rangle$ are, respectively, the initial and final states of the excited electron. In Eq. (9) (given in SI units), the matrix element is evaluated over the coordinates of all the atomic electrons, and the sum over all energy-degenerate initial and final states is implicitly assumed. In addition, it is assumed that only one scattering event occurs. Furthermore, $|f\rangle$ is a continuum wave function normalized per unit energy, i.e.,

$$\int_0^\infty |\langle f_E|f_{E'}\rangle|^2 r^2 dr=\delta(E-E') . \quad (10)$$

Although Eq. (9) is based solely upon considerations of atomic scattering, calculations for excitations of core electrons have successfully reproduced the overall edge shapes observed in the energy-loss spectra of solids.[30,31]

Equation (9) may be generalized for use in calculations of the fine structure at ionization edges due to solid-state effects. In this case it is necessary to replace the sum over the degenerate, continuum states with a density of final states representative of the solid.[32] As the core (initial) electron states are filled, only the density of final states must be considered. This generalization gives

$$\frac{d\sigma}{dE}=\frac{8\pi\hbar^2}{a_0^2 m_0^2 v^2}n(E)\int_{q_{\min}}^{q_{\max}}\frac{1}{q^3}|\langle f|e^{i\mathbf{q}\cdot\mathbf{r}}|i\rangle|^2 dq . \quad (11)$$

In Eq. (11), the wave functions are those appropriate to the solid.

Using Eq. (11), Weng, Rez, and Sankey[33] calculated the near-edge structure at the K and L absorption edges of a number of compounds with good accuracy. The one-electron, initial-state wave functions were obtained from Hartree-Slater calculations, while the density of states and final-state wave functions were obtained from pseudoatomic-orbital band-structure calculations. In similar work Müller, Jepsen, and Wilkins[34] calculated the fine structure at the K, L, and M edges for some of the $3d$ and $4d$ transition metals using a linearized, augmented, plane-wave method and obtained good agreement with observed spectra.

Our calculations of the normalized white-line intensities were also based upon Eqs. (9) and (11). First, the white-line contribution (excitations to unoccupied $3d$ and $4d$ states) was calculated using one-electron, Hartree-Slater[35,36] wave functions generated with the computer code of Herman and Skillman.[37] The code was configured to iterate until the potential was consistent to 0.1%. The continuum intensity was then calculated in a region from 50 to 100 eV past the L_3 edge threshold. The calculated white-line contribution was then divided by the calculated continuum intensity yielding a normalized white-line intensity. The continuum wave functions for the calculation were generated by directly integrating the Schrödinger equation on a linear grid using the self-consistent potential obtained from a Hartree-Slater calculation. The wave functions were normalized so their amplitude at $40a_0$ (essentially infinity) was $\pi^{-1/2}\varepsilon^{-1/4}$, where ε is the continuum energy in Rydbergs.[38] Wave functions were recalculated using successively smaller grid spacings down to $0.001a_0$ to check the convergence of the integrations. The maximum difference between wave functions calculated on the 0.001 grid and 0.002 grid was less than 0.1% of the maximum amplitude. The bound-state wave functions are expected to have comparable uncertainties as the Herman-Skillman code calculates these wave functions using a similar linear grid spacing of $0.0025a_0$ at small r.

In the limit $q \rightarrow 0$, only dipole transitions contribute to the matrix elements, but at nonzero q higher-order transitions also contribute. Calculations of $L_{2,3}$ spectra that include these higher-order transitions have shown, however, that they become significant only at energies several hundred eV past the edge onset.[39,30] For this reason, only dipole transitions were considered in the calculations presented here. In addition, only transitions to final states with d symmetry were considered, since transitions to states with s symmetry were found to be negligible in comparison. Furthermore, our intent was to evaluate the *ratio* of the white line to continuum contribution, rather than to calculate absolute intensities, so the integrals over q were ignored. Under these assumptions, the normalized white-line intensity is approximately

$$I \approx n_d \frac{|\langle 3d(\text{or } 4d)|r|2p\rangle|^2}{\int_{50}^{100} |\langle \varepsilon d|r|2p\rangle|^2 d\varepsilon} = n_d \frac{M_{\text{white line}}}{M_{\text{continuum}}} , \quad (12)$$

where n_d is the number of d holes, εd is a continuum state with energy ε and $l=2$, and the radial matrix elements are as indicated.

Calculations of the white-line matrix elements were carried out using electronic configurations representative of the solid with the addition of a $2p$ core hole (excited-state configuration). The electron removed from the $2p$ shell was placed in the outer d shell, resulting in a $2p^5d^Ns^1$ configuration. Here, N is the total number of s and d valence electrons. The continuum matrix elements were also calculated using excited-state configurations. In this case, the Hartree-Slater problem was solved for an ion with a $2p$ core hole, and the continuum wave function was then calculated from the resulting self-consistent potential. In addition, rather than evaluate the denominator of Eq. (12) by integrating over closely spaced energies from 50 to 100 eV, this term was approximated by linear interpolation of the 50- and 100-eV matrix elements as the matrix elements were found to vary slowly with energy. Examples of the calculated radial wave functions are shown in Fig. 7 for Ni. The $2p$ and $3d$ wave functions are those for the atom with the core hole, and the continuum wave function is that for the ion with the core hole.

The calculations described thus far are strictly atomic in nature. Solid-state effects may be taken into account approximately by renormalizing the $3d$ and $4d$ radial wave functions for the various atoms within their appropriate Wigner-Seitz spheres.[40] No correction is necessary for the $2p$ wave functions, as they already lie well within the Wigner-Seitz radius. Normalized white-line intensities were calculated using both renormalized and standard atomic wave functions. In the calculations for the $3d$ metals, the continuum window intensity was multiplied by 1.5 to account for the L_2 edge contribution to the experimental background intensity. In addition, the uncertainties in the intensities calculated according to Eq. (12) were estimated by propagating the uncertainties in the radial wave functions. Error calculations were carried out for metals at the beginning and end of each transition series and were found to be ±2% for Ti, ±4% for Ni, ±5% for Zr, and ±2% for Pd.

Comparisons between the calculations and the data are presented in Figs. 8 and 9 for $3d$ and $4d$ transition metals,

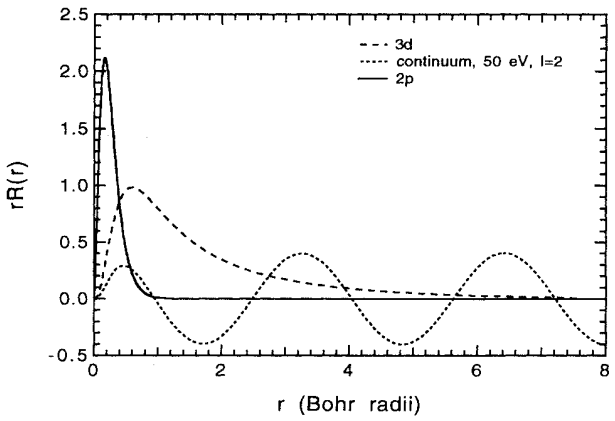

FIG. 7. Hartree-Slater radial wave functions for Ni.

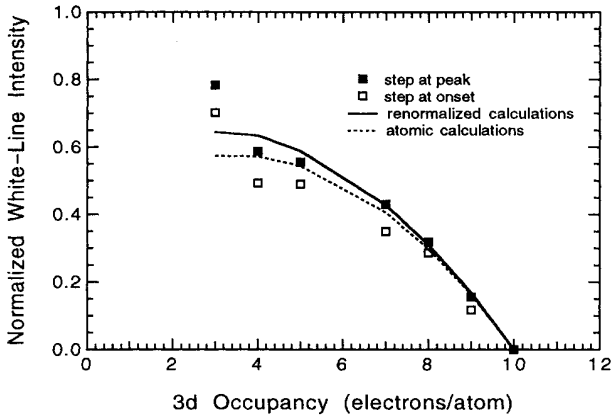

FIG. 8. Comparison of calculated and experimental normalized white-line intensities for the 3*d* transition metals.

respectively. Both the renormalized and the strictly atomic calculations have been presented to illustrate the magnitude of the renormalization correction.

V. DISCUSSION

As shown in Fig. 8 for the 3*d* metals, good agreement was obtained between the renormalized calculations and the data generated by placing the step functions at the white-line peaks. In Fig. 9, for the 4*d* metals, the renormalized calculations again more closely follow the data generated by placing the step functions at the white-line peaks, but significant deviations are observed for Zr and Nb. It is not obvious at present if these discrepancies result from inadequacies in the atomic nature of the calculations, or from the step functions providing a poor method for isolating the white-line intensities, or perhaps both. As mentioned earlier, solid-state calculations of the edge profile resolved according to final angular momentum states could provide a more accurate method for isolating the white lines.

We used these calculations to correct our experimental data for the effects of the matrix elements, thereby obtaining correlations more appropriate for measuring

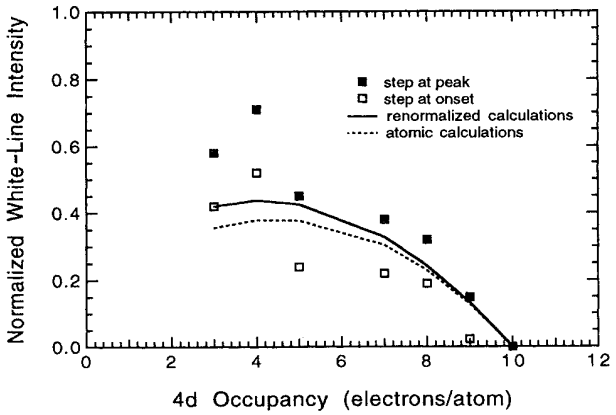

FIG. 9. Comparison of calculated and experimental normalized white-line intensities for the 4*d* transition metals.

TABLE I. Matrix-element correction factors for the 3*d* and 4*d* transition metals.

Metal	$\frac{M_{\text{white line}}}{M_{\text{continuum}}}$
Ti	0.0921
V	0.106
Cr	0.118
Fe	0.143
Co	0.155
Ni	0.169
Cu	0.172
Zr	0.0600
Nb	0.0729
Mo	0.0851
Ru	0.109
Rh	0.122
Pd	0.134
Ag	0.141

changes in *d*-state occupancy. The correction involves dividing the experimental data points of Figs. 8 and 9 by $M_{\text{white line}}/M_{\text{continuum}}$ from the right-hand side of Eq. (12). These matrix element factors, calculated using renormalized wave functions, are presented in Table I. The matrix element factors for Cu and Ag were calculated using $2p^6d^{N-1}s^1$ configurations (i.e., no core hole) since the outer *d* states in these metals are already filled.

Figure 10 shows the experimental, normalized white-line intensities for the 3*d* transition metals after correcting for the variation in the transition matrix elements for different atoms. Data obtained by positioning the step functions at the peaks and at the onsets are represented by solid squares and open squares, respectively, and the respective linear fits to the data are given by

$$I'_{3d}=10.8(1-0.10n_{3d}) \text{ for steps at peaks} \quad (13)$$

and

$$I'_{3d}=9.4(1-0.10n_{3d}) \text{ for steps at onsets.} \quad (14)$$

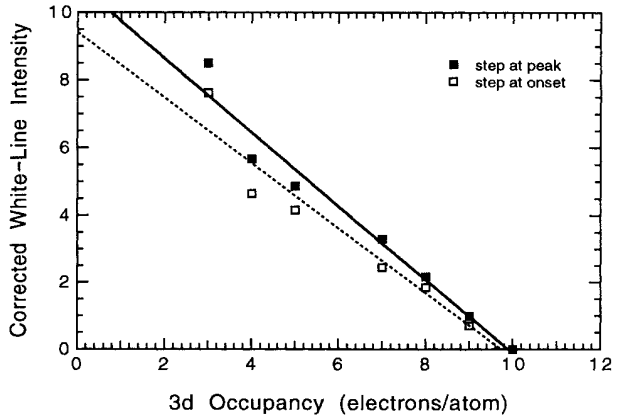

FIG. 10. Plot of experimental white-line intensity for the 3*d* transition metals corrected for the variations of the radial matrix elements. Linear fits to the data give $I=10.8(1-0.10n)$ for the upper curve (steps at peaks) and $I=9.4(1-0.10n)$ for the lower curve (steps at onsets).

The factors of 0.10 are in excellent agreement with that in Eq. (4). In addition, the leading constant in Eqs. (13) and (14) is no longer arbitrary and should, in fact, be 10, since dividing out the matrix elements should make the normalized white-line intensity equal to the number of d holes. The corresponding data for the $4d$ metals is shown in Fig. 11. Linear fits to the data yield

$$I'_{4d}=14.0(1-0.10n_{4d}) \quad \text{for steps at peaks} \qquad (15)$$

and

$$I'_{4d}=10.0(1-0.11n_{4d}) \quad \text{for steps at onsets} . \qquad (16)$$

The correlations in Fig. 10 for the $3d$ metals appear good enough to consider using them to estimate d-occupancy changes that might occur, for example, during alloying. Using the upper curve (these data more closely fit the calculations as shown in Fig. 8), one first divides the change in normalized white-line intensity by the appropriate matrix element factor from Table I and then applies Eq. (13). For example, if the Cu $L_{2,3}$ edge in a Cu alloy displays an enhancement in the normalized white-line intensity of $+\Delta I$ compared to the pure metal, we obtain $\Delta n=\Delta I/[(0.172)(10.8)(-0.10)]$. It should be pointed out that such a measurement only provides an estimate of the net change in d count (as defined in Sec. III) for a given atom species. The measurement does not provide an indication of whether this change results from a transfer of d electrons or from hybridization.

As mentioned earlier, previous studies obtained the proportionality between d-state occupancy and white-line intensity through band-structure calculations of d-state occupancies for a few pure metals. Such an approach, however, suffers from uncertainties in isolating small white-line intensities for the late transition metals, and from inaccuracies in the calculations. The approach presented here provides an alternative method, as the proportionality between white-line area and d-state occupancy is not solely dependent upon one metal, but is determined by analyzing the systematics across the entire series. Furthermore, the previous studies simply would not allow measurements on Cu alloys, since there is no white in the pure metal from which to develop the proportionality between d holes and white-line intensity. Measurements on a number of Cu alloys will be presented in a forthcoming paper.

VI. CONCLUSIONS

We have performed an experimental study on the white lines from $L_{2,3}$ EELS spectra for elemental metals of the $3d$ and $4d$ transition series. The normalized intensities of these white lines were found to decrease nearly linearly with increasing d-state occupancy across each series. In addition, we modeled this normalized, white-line intensity using atomic, one-electron, Hartree-Slater calculations. Solid-state effects were taken into account approximately by renormalizing the outer d-state wave functions within their Wigner-Seitz spheres. Calculations were in excellent agreement with experiment except for the early $4d$ transition metals. Correcting the normalized white-line intensities for the effects of the matrix elements provides a method for measuring changes in d-state occupancy given an observed change in the normalized white-line intensity.

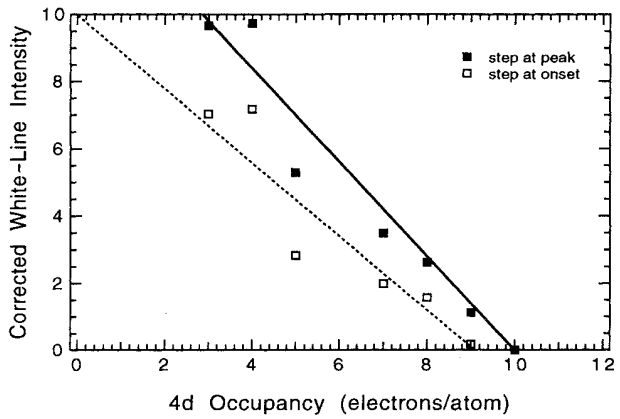

FIG. 11. Plot of experimental white-line intensity for the $4d$ transition metals corrected for the variations of the radial matrix elements. Linear fits to the data give $I=14.0(1-0.10n)$ for the upper curve (steps at peaks) and $I=10.0(1-0.11n)$ for the lower curve (steps at onsets).

ACKNOWLEDGMENTS

We thank Dr. Peter Rez of Arizona State University for useful discussions. This work was supported by the United States Department of Energy under Contract No. DE-FG03-86ER45270. The TEM facility was supported by the National Science Foundation under Grant No. DMR-8811795. The Gatan 666 EELS spectrometer was acquired through an equipment grant from Caltech's Program in Advanced Technologies, supported by Aerojet General, General Motors, and TRW.

*Present address: U.S. Naval Research Laboratory, Materials Science & Technology Division, Code 6371, 4555 Overlook Ave., S. W., Washington, DC 20375.

[1]N. F. Mott, Proc. R. Soc. London **62**, 416 (1949).
[2]J. Veldkamp, Physica **2**, 25 (1935).
[3]F. W. Lytle, P. S. P. Wei, R. B. Greegor, G. H. Via, and J. H. Sinfelt, J. Chem. Phys. **70**, 4849 (1979).
[4]J. A. Horsley, J. Chem. Phys. **76**, 1451 (1982).
[5]A. N. Mansour, J. W. Cook, and D. E. Sayers, J. Phys. Chem. **88**, 2330 (1984).
[6]T. K. Sham, Phys. Rev. B **31**, 1903 (1985).
[7]T. K. Sham, Solid State Commun. **64**, 1103 (1987).
[8]T. K. Sham, K. H. Tan, and Y. M. Yiu, Physica B **158**, 28 (1989).
[9]M. Brown, R. E. Peierls, and E. A. Stern, Phys. Rev. B **15**, 738 (1977).
[10]L. F. Mattheiss and R. E. Dietz, Phys. Rev. B **22**, 1663 (1980).
[11]R. D. Leapman and L. A. Grunes, Phys. Rev. Lett. **45**, 397

(1980).
[12]J. Zaanen, G. A. Sawatzky, J. Fink, W. Speier, and J. C. Fuggle, Phys. Rev. B **32**, 4905 (1985).
[13]W. G. Waddington, P. Rez, I. P. Grant, and C. J. Humphreys, Phys. Rev. B **34**, 1467 (1986).
[14]T. I. Morrison, M. B. Brodsky, and N. J. Zaluzec, Phys. Rev. B **32**, 3107 (1985).
[15]D. M. Pease, S. D. Bader, M. B. Brodsky, J. I. Budnick, T. I. Morrison, and N. J. Zaluzec, Phys. Lett. **114A**, 491 (1986).
[16]E. A. Stern and J. J. Rehr, Phys. Rev. B **27**, 3351 (1983).
[17]D. H. Pearson, B. Fultz, and C. C. Ahn, Appl. Phys. Lett. **53**, 1405 (1988).
[18]D. W. Johnson and J. C. H. Spence, J. Phys. D **7**, 771 (1974).
[19]R. F. Egerton, *Electron Energy-Loss Spectroscopy in the Electron Microscope* (Plenum, New York, 1986), pp. 259–261.
[20]H. Shuman and P. Kruit, Rev. Sci. Instrum. **56**, 231 (1985).
[21]R. F. Egerton and M. J. Whelan, Philos. Mag. **30**, 739 (1974).
[22]J. C. Fuggle, F. U. Hillebrecht, R. Zeller, Z. Zolnierek, P. Bennett, and Ch. Freiburg, Phys. Rev. B **27**, 2145 (1982).
[23]M. Grioni, J. B. Goedkoop, R. Schoorl, F. M. F. de Groot, J. C. Fuggle, F. Schäfers, E. E. Koch, G. Rossi, J. M. Esteva, and R. C. Karnatak, Phys. Rev. B **39**, 1541 (1989).
[24]N. F. Mott, Adv. Phys. **13**, 325 (1964).
[25]H. Danan, A. Herr, and A. J. P. Meyer, J. Appl. Phys. **39**, 669 (1968).
[26]L. Hodges, H. Ehrenreich, and N. D. Lang, Phys. Rev. **152**, 505 (1966).
[27]D. G. Pettifor, J. Phys. F **7**, 613 (1977).
[28]H. A. Bethe, Ann. Phys. **5**, 325 (1930).
[29]M. Inokuti, Rev. Mod. Phys. **43**, 297 (1971).
[30]R. D. Leapman, P. Rez, and D. F. Mayers, J. Chem. Phys. **72**, 1232 (1980).
[31]C. C. Ahn and P. Rez, Ultramicroscopy **17**, 105 (1985).
[32]S. T. Manson, in *Photoemission in Solids I. General Principles,* edited by M. Cardona and L. Ley, Topics in Applied Physics Vol. 26 (Springer-Verlag, New York, 1978), pp. 135–163.
[33]X. Weng, P. Rez, and O. F. Sankey, Phys. Rev. B **40**, 5694 (1989).
[34]J. E. Müller, O. Jepsen, and J. W. Wilkins, Solid State Commun. **42**, 365 (1982).
[35]J. C. Slater, Phys. Rev. **81**, 385 (1951).
[36]D. R. Hartree, *The Calculation of Atomic Structures* (Wiley, New York, 1957).
[37]F. Herman and S. Skillman, *Atomic Structure Calculations* (Prentice Hall, Englewood Cliffs, 1963).
[38]R. D. Cowan, *The Theory of Atomic Structure and Spectra* (University of California Press, Berkeley, 1981), p. 515.
[39]J. K. Okamoto, D. H. Pearson, C. C. Ahn, and B. Fultz, in *Applications of Transmission EELS in Materials Science,* edited by M. M. Disko, C. C. Ahn, and B. Fultz (The Metallurgical Society, Wanendale, PA, 1992), pp. 183–216.
[40]L. Hodges, R. E. Watson, and H. Ehrenreich, Phys. Rev. B **5**, 3953 (1972).